LASER INTERFEROMETER GRAVITATIONAL WAVE OBSERVATORY
- LIGO -
CALIFORNIA INSTITUTE OF TECHNOLOGY
MASSACHUSETTS INSTITUTE OF TECHNOLOGY

Document Type	**LIGO-T0900112-v1-H**	2009/03/13

Seismic studies at the Homestake mine in Lead, South Dakota

J. Harms (janosch@physics.umn.edu)
A. Sajeva (angelo.saje@gmail.com)
T. Trancynger (tom.trancynger@state.sd.us)
R. DeSalvo (desalvo@ligo.caltech.edu)
V. Mandic (mandic@physics.umn.edu)

Distribution of this draft:
Final
LIGO Scientific Collaboration

California Institute of Technology
LIGO Project - MS 51-33
Pasadena CA 91125
Phone (626) 395-2129
Fax (626) 304-9834
E-mail: info@ligo.caltech.edu

Massachusetts Institute of Technology
LIGO Project - MS 20B-145
Cambridge, MA 01239
Phone (617) 253-4824
Fax (617) 253-7014
E-mail: info@ligo.mit.edu

WWW: http://www.ligo.caltech.edu/

Processed with LaTeX on 2009/03/13

1 Introduction

In the future, ground-based gravitational-wave detectors are likely to probe frequencies below 10 Hz which marks the lower boundary of the detection band of surface GW detectors like Advanced LIGO. One contribution to the instrumental noise at low frequencies is the gravity-gradient noise. The instruments cannot be shielded from gravity-gradient noise, also known as Newtonian noise, which exerts a fluctuating force on the suspended test masses through variations in the gravity field. Time variations in the gravity field at the position of the test masses are generated by seismic noise induced density fluctuations in the vicinity of the detector. We believe that a combination of measures could considerably reduce the Newtonian-noise contribution to the interferometer data stream. The first step is to identify a location where density fluctuations are as weak as possible. Since density variations are determined by certain modes of the seismic-wave field, a good location can be found by carrying out a seismic survey comparing results from various locations. Second, if a model was found which linked the gravity-gradient noise to data produced by a 3D network of seismometers around the detector, then it would be possible to use the seismometer data to calculate with some precision the gravity-gradient noise and subtract it from the data.

These two measures motivated our design of a seismic study. It is known that in underground environments, absence of surface modes leads to decreased seismic noise and therefore decreased density fluctuations. For several reasons, the former Homestake mine in Lead, South Dakota, was a very promising candidate to carry out our measurements. In January 2002, the Barrick Gold Corporation ceased operation of the mine which was then donated to the state of South Dakota. It is being transformed gradually into a scientific laboratory controlled by the South Dakota Science and Technology Authority (SDSTA). The endeavor is supported by a private gift from Mr. Sanford and to a smaller extent by the NSF. The Homestake mine is now known as the Sanford Laboratory. It lies far from the oceans and has the deepest reaching tunnels in North America (8000 ft) which provides an optimal stage for monitoring the seismic noise with a three dimensional network of seismometers.

Between July 21 and September 26, 2008, we conducted our first series of seismic measurements on various underground levels in the Homestake mine. Our goal was to familiarize with the working procedures in a mine, to learn how to set up an experiment in underground conditions and to obtain first results from a small array of seismometers. Here, we report on our experiences and summarize the results. We worked on three different levels starting with the 300 ft level and then continuing with the 2000 ft and 800 ft level. At that time, other levels at greater depths were not accessible. Data was collected from a Streckeisen STS-2 and two Trillium 240. More recently, a Güralp CMG-40T joined the network. This experiment is intended as a starting point for a more exhaustive survey, to take place over the next few years, with the aim to ascertain to which level Newtonian noise can be reduced or subtracted from the data stream, and to which level and to which frequency we can extend the sensitivity of underground GW observatories.

The report is organized as follows. A brief description of the local Homestake geology is given in section 2. The infrastructure of the laboratory is presented and general environmental conditions are outlined in section 3. Safety procedures as outlined in section 4 greatly affected our work and they formed a vital part of daily procedures. The construction of the three seismic stations is described in section 5. In section 6, we give a brief description of the instrumentation which includes the seismometers, environmental monitors and the DAQ system. In section 7, the report concludes with a brief summary of new developments which will be presented in detail in a following report.

2 Geology of the Lead Window

The Homestake mine became famous as the largest known iron-formation-hosted gold-ore body in the world and is considered as the prototype of its kind. It is situated in the Lead-Deadwood Dome of the Black Hills which is marked by a rather complicated stratification and history of folding events and metamorphosis of igneous and sedimentary rocks. Two uplifts have brought the Black Hills into its present domal configuration. A first event about 2 billion years ago, in the Proterozoic during the Trans-Hudson orogeny exposed a sequence of Archean and early Proterozoic rock strata. This event was accompanied by (syndeformational) regional metamorphosis of the early Proterozoic sedimentary and volcanic rocks into lower-greenschist to middle-amphibolite facies. New sediments

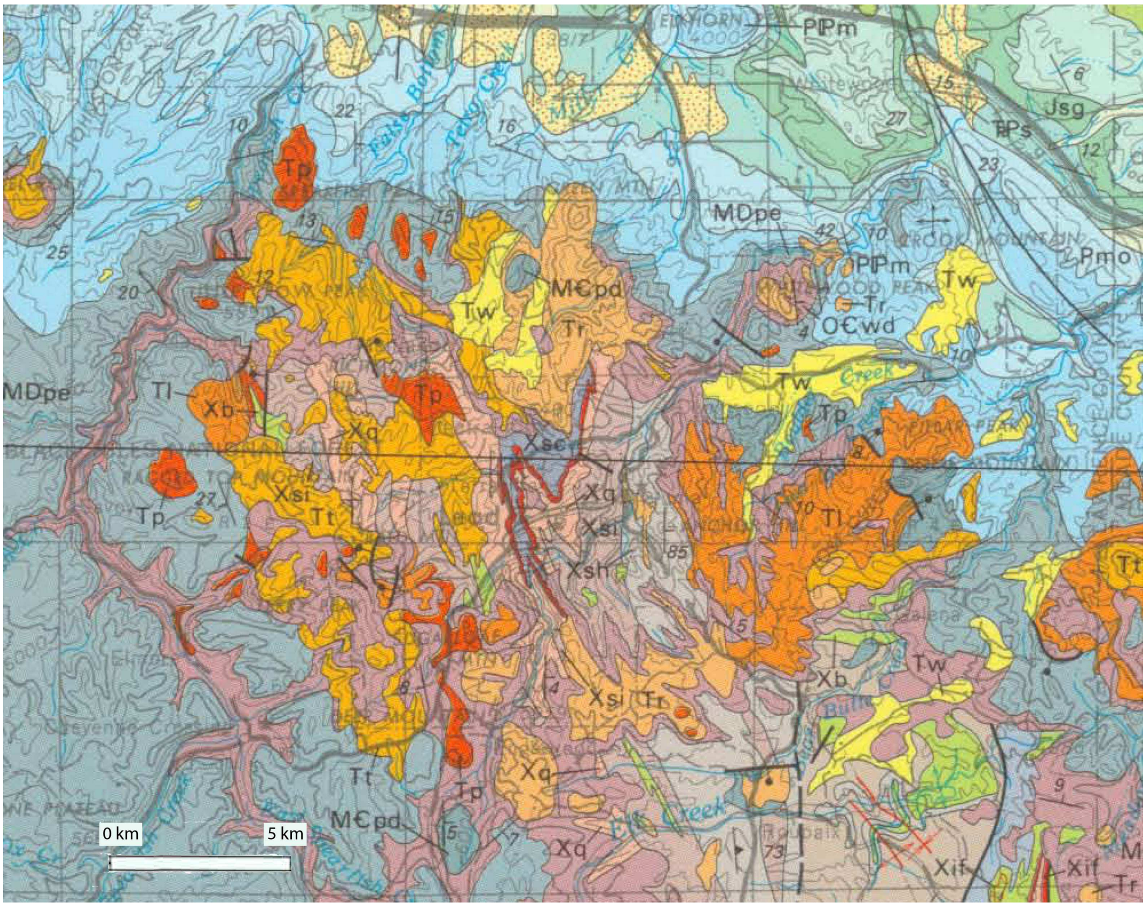

Figure 1: Geologic map of the Lead-Deadwood Dome [1]. Two or three letters are used to identify each rock type. The first letter indicates the age of the rock (X: Proterozoic, T: Tertiary, other ages are irrelevant here). The remaining letter(s) further specify the rock type or formation (e.g. Xif: iron formation, Xsc: metamorphosed carbonaceous shale, Xsi: metamorphosed siltstone, Xq: quartzite, Tp: phonolitic intrusive rock, Tt: trachytic intrusive rock). Note that the red-colored line in the center also indicates an iron-formation rock (Xif) which is better known as the Homestake formation.

were deposited in the Paleozoic and Mesozoic eras during a period of relative tectonic quiescence until a second uplift of the Black Hills area (65 - 60 million years ago) during the Laramide orogeny occurred, followed by alkalic igneous intrusion of laccoliths, dikes and sills into the preexisting

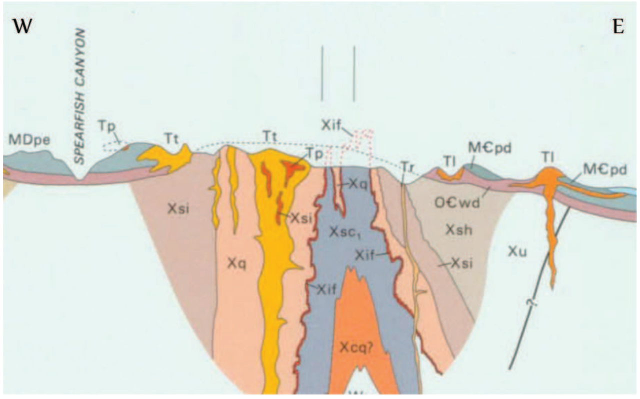

Figure 2: West-East cross section through Homestake geology along the almost horizontal line through the middle of figure 1.

strata of the northern Black Hills. This last partially brittle phase of deformation is responsible for a network of fractures which facilitates the influx of meteoric water into the Homestake mine as mine workings and diamond-drill holes intersect these watercourses. Figure 1 shows the geology of the Lead-Deadwood Dome. Of special interest is the center of the map which contains a fold structure indicated by a relatively thin red line which marks a Proterozoic iron formation. Locally, the (blue) formation within the fold limbs is often denoted by Xp which stands for Poorman formation and the (pink) formation outside the limbs is known as the Ellison formation Xe. The iron formation itself is the Homestake formation Xh which hosted the gold-ore bodies. The Poorman formation is the oldest, then comes the Homestake formation and finally the Ellison formation. The vertical cut through the Homestake geology, figure 2, reveals a clearer pattern of the underlying stratification. The (blue) Poorman formation lies right of the fold structure whereas the Ellison formation shown in pink is the outermost layer of the mine area. If older rocks are found within a fold, then it is called an anticline. If the younger rock is enclosed by the limbs, then the fold is called a syncline. The fold structure actually consists of two anticlines and one syncline as can be seen in figure 1 (the iron formation has a w-shape). The Poorman formation is generally 1500 m thick. Before deformation, the Homestake formation used to be 20-30 m thick, but distortion thinned it out to zero thickness at some places or it thickened to 150 m, especially at the hinges of the folds. Due to stratigraphic ambiguities, the thickness of the Ellison formation is not well determined. In the mine area it does not exceed 400 m [4]. The entire rock package at the Homestake mine was subjected to several periods of deformation resulting in complex fold patterns and localized shear zones. A zoom onto the Homestake area shows a system of smaller-scale synclines and anticlines imprinted on the Homestake formation (see figure 3). These folds are termed "ledges" and are numbered from East to West. The odd-numbered ledges correspond to synclines which are the ore ledges of the mine, and the even-numbered ledges are anticlines respectively. Among the first synclines, the Main Ledge and Caledonia Ledge have their own name. The Main Ledge was mined underground and in an open cut (see figure 4) producing most of the gold. Ten ore ledges have produced gold:

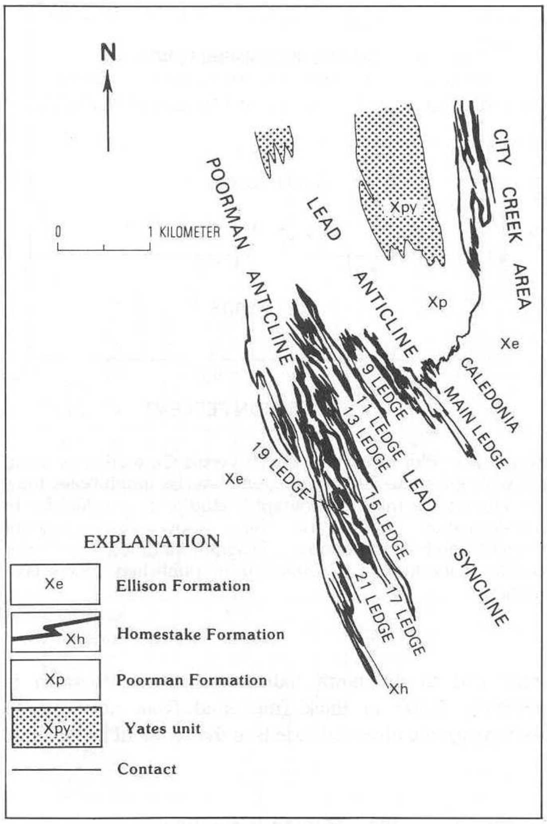

Figure 3: Geology of 2600 level of the former Homestake mine, showing fold structures and ledges [4].

Figure 4: The open cut of the Homestake mine.

Caledonia, Main, 7, 9, 11, 13, 15, 17, 19, 21 Ledges. As mentioned before, a complex syndeformational series of prograde metamorphic processes took place and imposed additional structure onto the folds which means that the rock type (metamorphic grade) varies within each of the three formations. Figure 5 displays a surface map of the Homestake geology indicating metamorphic zones [3]. The highest grade metamorphosed rock is found as middle amphibolite facies at the North-East corner and was created at about $630°$C. The lowest grade metamorphosed rock is found in lower greenschist facies to the West which was created at temperatures around $370°$C. An "X" isograd marks the first appearance of the mineral X following a NNW direction. Here, garnet and staurolite were used as indicators of metamorphic grade. The base of the Poorman formation, sometimes called Yates unit, consists of metamorphosed tholeiitic basalts in the form of amphibolites (hornblende-plagioclase schist). Tholeiitic basalts are the most common volcanic rocks on Earth. The type includes basalts produced by submarine volcanism at mid-ocean ridges which make up much of the ocean crust. It is relatively poor in silica and alkali oxides. Most samples from the Yates unit are derived from oceanic basalts (higher TiO_2 content than continental tholeiitic basalts). The remaining Poorman lithologies are carbonate-rich metasediments (sedimentary rock which shows evidence of metamorphism) including a complex succession of rock types of sericite- and biotite-rich carbonate, quartz-bearing phyllite and graphitic phyllite. The Poorman formation has a lower and upper metasedimentary unit, the latter being less than 1 m to 30 m thick. Poorman metasediments are interpreted as chemical precipitates deposited in a low-energy environment of a shallow to intermediate-depth oceanic basin. Within the Homestake iron formation, an abundance of siderite (iron carbonate) phyllite in upper greenschist facies develops into a grunerite (iron-rich inosilicate) schist abundance in lower amphibolite facies. The metamorphic reaction from siderite to grunerite is accompanied by devolatilization of carbon dioxide. Therefore, depending on the location of the mine, the Homestake formation is either carbonate or silicate dominated. The overlying Ellison formation consists of interbedded strata of phyllite, quartz-mice schist and quartzite. Their protoliths have been interpreted as shale, impure siltstone and

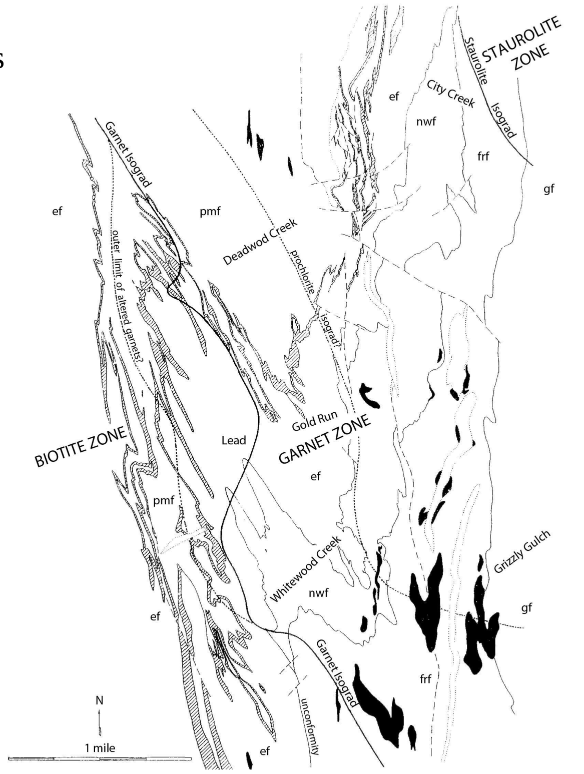

Figure 5: Isograds of the metamorphic transformation [3].

sandstone respectively deposited in a constructive or lobate delta where fluvial action and depositional processes dominate the system. It should be clear that many details of the geology will be measurable by a network of seismometers. People have applied seismic techniques in the past to obtain information about crystallography and rock structures throughout the world. These investigations focused on seismic waves produced by explosions and earthquakes. A dense three dimensional network of seismometers would provide much more detail on smaller scales extracted from correlations between different locations. The situation is opposite at Homestake: since a geologic map of the Homestake rock already exists, it can be used to understand certain features of the correlation data.

3 Infrastructure of the Homestake mine

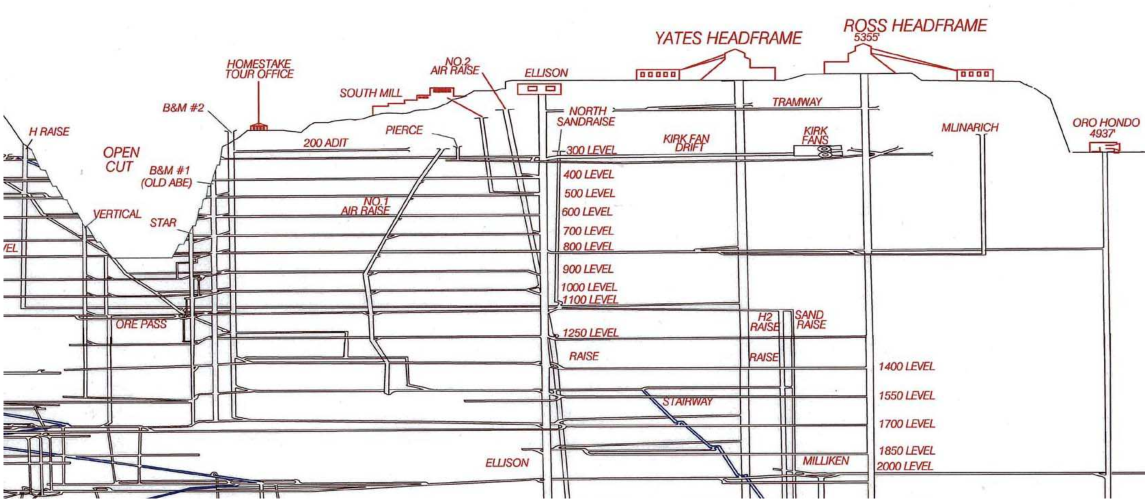

Figure 6: Projection of the upper Homestake mine workings onto a vertical plane whose normal is oriented towards the North-East direction. Currently, access to all underground levels is through the Ross shaft. Reactivation of the Yates shaft is currently being prepared.

The main units of mine workings are the shafts, winzes, raises, drifts, cross-cuts and stopes. Shafts are vertical tunnels which are connected to the surface whereas winzes are vertical tunnels which connect underground levels only. Winzes are usually called raises when they are inclined. Horizontal tunnels are drifts if they are driven parallel to the rock fabric, otherwise they are called cross-cuts. Finally, a stope is a mined-out ore body. Stopes are refilled with waste rock to stabilize the mining volume. A miner derives names for the wall and ceiling of a tunnel by comparing it with the internal view on an animal. The ceiling is the back and the walls are the ribs. People at Homestake call the ground the sill which has nothing to do with the geological term. In the following, we show sketches of the 300 ft, 800 ft and 2000 ft levels. The actual size of each level can be much larger than the displayed part which was chosen to contain the Ross shaft (which is currently the main access to all levels) and the location of our seismic site. Teams are currently preparing reactivation of the Yates shaft by exchanging the partially wooden support structure by a metal support. The sea level coincides with the 5400 ft depth of the mine.

In the following, we present maps of the three levels (figures 7-9) which include contours of the

Homestake formation, which is also the interface between the Poorman (NW) and Ellison (SE) formations. With increasing depth, this interface advances towards the South-East. Therefore, whereas the 300 ft station lies well inside the Ellison formation, the 2000 ft station lies deep inside a structurally complex environment which includes all three formations. It is to be expected that a correlation measurement between different sites will depend on these large-scale structures (i.e. discontinuous phase and amplitude changes at formation interfaces). The Sanford Lab owns an extensive database of rock samples which can be used to calculate profiles of rock density and other relevant parameters and derive a testable model for seismic correlations.

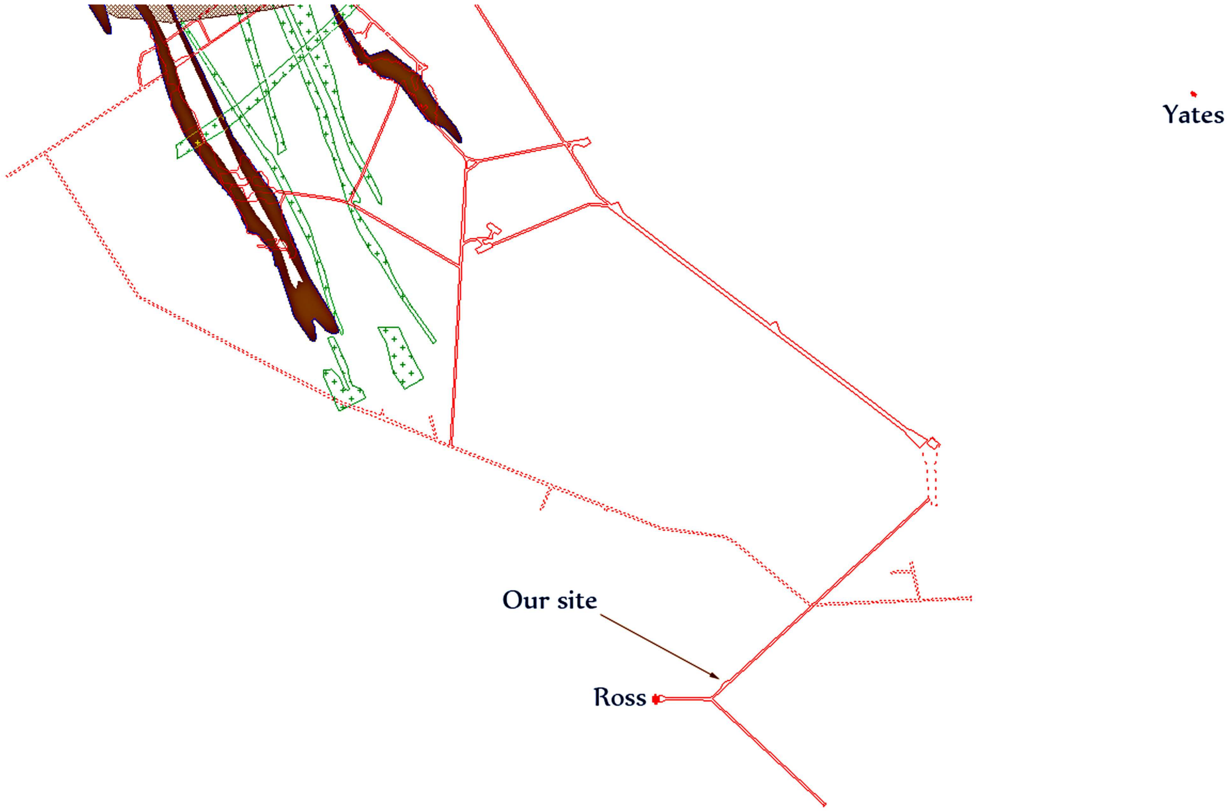

Figure 7: Sketch of the 300 ft level. The filled contours represent the Homestake formation. Both shafts (at this level) and our site are part of the Ellison formation. The brown-shaded contour in the North-West is the southern part of the open cut. The green contours correspond to younger rhyolite intrusions. Most of the mine workings are currently not accessible to scientists and miners. For security reasons, many drifts and stopes were filled back with waste rock. The distance between the Ross shaft and our site is about 250 ft.

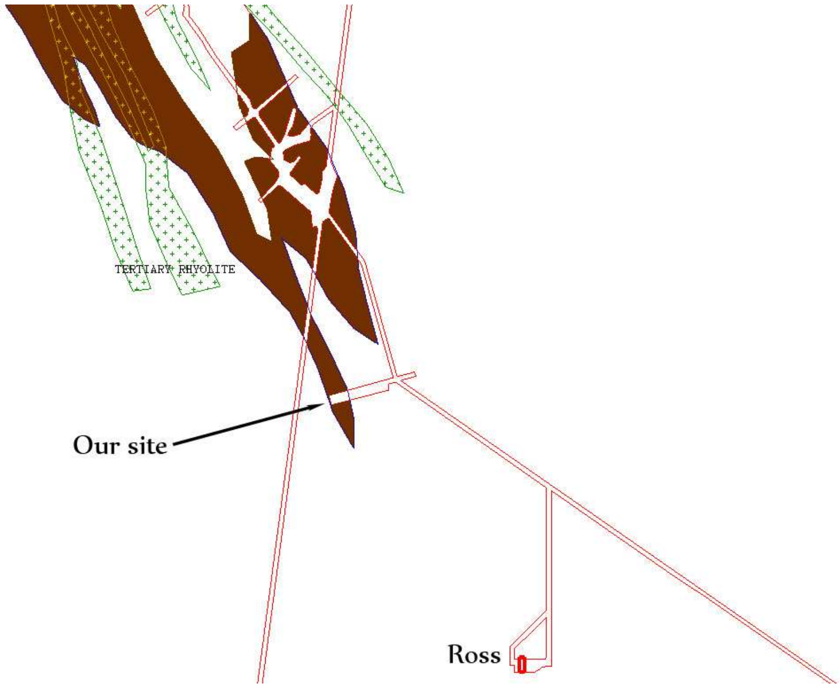

Figure 8: Sketch of the 800 ft level. The Homestake formation advances to the South-East direction with increasing depth. Our site is situated right inside a tip of a ledge. The distance between the Ross shaft and the site is about 600 ft.

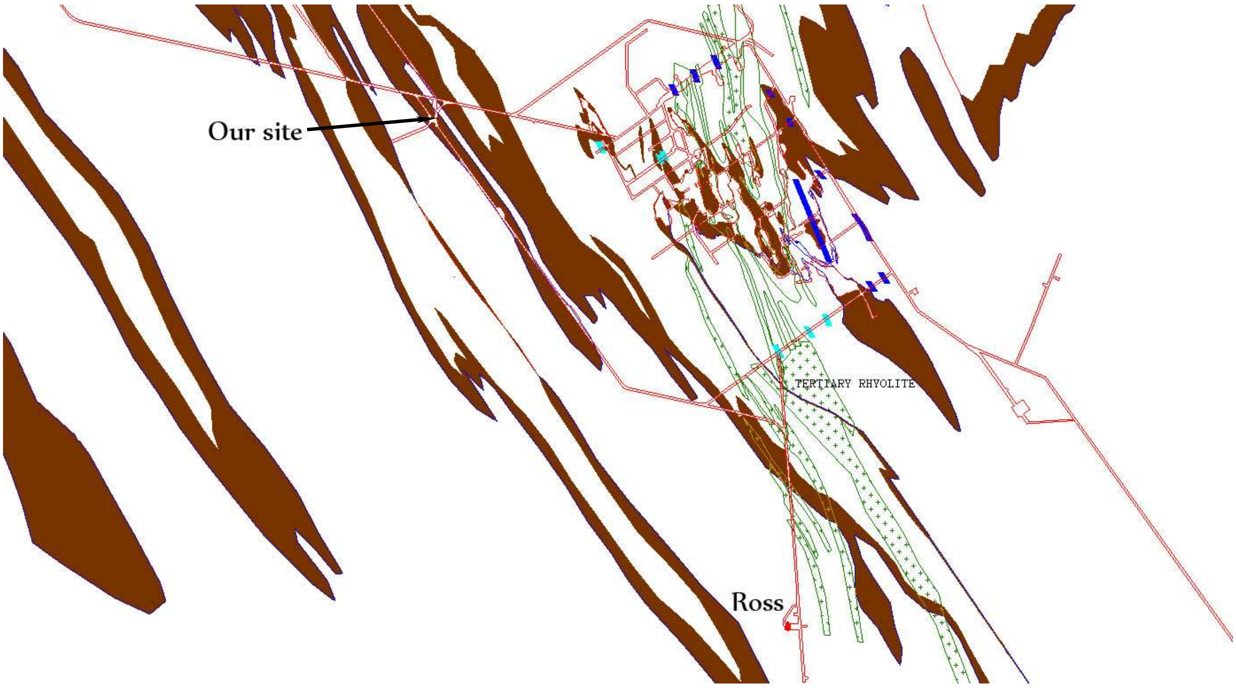

Figure 9: Sketch of the 2000 ft level. Like on the preceding two figures, the filled contours represent the Homestake formation. The (walking) distance between our site and the Ross shaft is about 2600 ft. End of October, old rail tracks between the shaft and the site have been reactivated and can be used to transport people and load with a motor.

4 Safety procedures and flow of work

Safety procedures at Homestake are taken very seriously and have been developed since decades. Already at times when Homestake was still operating as a gold mine, it had an excellent reputation in terms of safety. People who plan to work underground for a long time have to attend a week-long safety class which is in addition to the site-specific training given to everyone who enters the mine (except for tourists who walk the tourist trail on the 300 ft level). As important as these safety classes are, the daily work inside the mine teaches more important lessons, and daily procedures had a significant impact on our science work and progress. In average, about 2 hours per day were dedicated to securing the working space and the paths between the sites. However, the amount of time decreases steadily once a site has been established. Most of this time is devoted to what is called barring down or scaling of rock. With a scaling bar, loose rock at the ribs or back is located and removed. Many chemical and physical processes can generate loose rock inside a mine. Oxidization is the main chemical reaction and takes place on rock surfaces and interfaces between rock layers. These chemical decompositions are supported by physical stress due to changing gravity fields (e.g. moon phases) and temperature drifts. Rock is loosened on timescales of a few weeks or shorter if it is scaled regularly. We have also participated in constructing supporting structures at places where the loose rock mass was too high to allow for scaling. The policy of the Sanford Lab demands that one experienced miner has to accompany science team at underground work. This summer, Tom Trancynger, a geologist who has been working at Homestake for more than thirty years, joined our team and supervised safety procedures and also helped us setting up the stations. All underground work has to be planned and formulated as an action plan which is signed by people in charge of safety and operation at Homestake. Any new material brought into the mine needs a material safety and data sheet (MSDS). Again, it was Tom Trancynger who prepared these documents for us.

Figure 10: Supporting structure at the 800 ft level.

The daily work flow underground follows a typical pattern. The team picks up the personal equipment at the Yates office building around 7.30am and meets the miner (i.e. Tom Trancynger) at 7.50am at the Ross shaft. Here, one has to tag in which means that one picks a numbered metal plate and leaves a copy of it at the surface attached to ones name. Like this, people at surface can always check who is underground if something happens and identify burned people underground by their metal tag. The shaft cage brings the team underground at 8am. Coming late usually means being forced to wait hours for the next opportunity to get a cage. The cage schedule used to be strictly enforced at times when Dynatec, a contractor which employed most miners, was in charge of installing power lines and pumping stations at levels near the water line (≈ 4530 ft in summer). Any extra cage time for scientists caused significant costs charged to SDSTA. The contract with Dynatec ended September 30 and the miners are now directly working for SDSTA which makes scheduling cage time more flexible. Still, using the cage beyond official cage times delays work of other teams in the mine and is not appreciated. This summer any science equipment had to be carried by hand, but since end of October a train is available to transport heavy loads and persons on various levels including the levels at 800 ft and 2000 ft. The team has to decide whether to stay underground for the entire day until 4.30pm when the working shift of the miners ends, or until lunch around 12.30pm. Returning to the surface, one has to tag out immediately.

Figure 11: Science team with personal-protection equipment.

5 Construction of experimental sites

Between July 21 and September 26, we constructed three sites for seismic measurements. A unique problem occurred at each construction site. It was the water at the 300 ft level, the web access at the 2000 ft level and the connection of the instruments to bottom rock at the 800 ft site. We had to create an isolated environment for the seismometers and additional sensors (details of the instruments will be given in section 6). The plan was to use polyurethane panels and foam to build a chamber which would provide a dry and stabilized atmosphere for the instruments. However, it turned out to be a little more complicated as will be outlined in sections 5.1 to 5.3. Common features of all three sites will be explained in the next section only. More details of the site constructions can be found in a supplementary LIGO document [2].

5.1 The 300 ft site

The 300 ft site was built between July 21 and August 21. A 110V AC power supply was available from the beginning and, as shown in section 3, the level can be accessed horizontally which greatly accelerates transportation of people and material. On the concrete platform of an old pumping station which was supposed to have good connection to bottom rock, we started building the instrument hut. Polyisocyanurate (PIR or ISO) panels in double layer were used to build the walls and roof. Polyurethane foam fills the gaps between panels and the ground and rock wall and acts as strong glue to fix the construction (see figure 12). The hope was that the foam sealant was waterproof and that a dehumidifer bucket placed inside the hut after drying the ground floor would be sufficient to dry the atmosphere so that instruments could be installed after a few days. It turned out to be insufficient. Drill holes around the pump station crosscut natural cracks in the rock (see section 2) and act as water channels. Especially during the rain season of the Black Hills, water flows in considerable amounts from the ribs (tunnel walls) and forms puddles on the concrete platform. The foam which connects the panels to the ground is a poor barrier against water. The consequence was that we could not prevent a small puddle to form inside the hut. As shown in figure 13, the next attempt was to build a second smaller PIR box inside the hut just large enough to host the instruments and a dehumidifier bucket. This measure brought some improvement, but it was still not good enough. The relative humidity (RH) inside the box was close to 100% as could be seen since drops formed all over the PIR box. Though a puddle did not form inside the box. The solution to the water problem was to elevate the ground around the panel walls inside and outside of the hut by adding a layer of concrete. A slope and channel system was built into the new concrete to optimize the drainage system. This, to the present day (Nov 11), has prevented puddels of significant size to form inside the hut and has created a completely dry atmosphere inside the PIR box (RH $\approx$ 75%). At the meantime, a second hut at about 4m distance to the instrument hut was constructed to host the DC power supply and the PC with our DAQ card. Shortly after construction of the site had been finished, one STS-2 and a sensor board were placed inside the instrument box and connected to the PC. The first data had to be retrieved manually, but a few weeks later, our own private local area network was established which allows communication between all PCs. In the beginning, the web link of the 300 ft station was provided by a pair of antennas which, mounted inside the Ross shaft, bridged the distance between the surface and the 300 ft level. The distance between the underground antenna and our site was small enough (< 328 ft) to allow an ethernet link between PC and antenna. The system was reliable and provided a fast link with small ping times between Ross Dry PC and 300 ft PC (< 3 ms with ping-time standard deviation below 0.3 ms). Therefore, the system would have been adequate to establish clock synchronization between different DAQ systems with sufficient precision (using a simple NTP demon). Nevertheless, the antennas were dismounted again, because the IT team of the SDSTA produced a wired connection to the three levels which host our instruments. Antennas in the shaft are also

Figure 12: Instrument hut at the 300 ft site.

Figure 13: Instrument box inside instrument hut.

prone to falling stones or ice during the winter and changes in the LAN settings could always make a dismount and remount of the antennas necessary which requires cage time and people who can work in the shaft, etc.

5.2 The 2000 ft site

The 2000 ft site was built between August 22 and August 29. As this location would stay our favorite station inside the mine for a long time with presumably lowest environmental noise and lowest seismic noise, we tried to be as careful as possible. The ground connection between bottom rock and concrete platform from an old charging station was checked and any audible source of dropping water was eliminated as good as possible. The 2000 ft level would be dry if the drainage system of the mine did not move water into (and out) of this level. This time, we had got a section of a tunnel which needed to be sealed from two sides with PIR panels. Similar to the walls of the instrument hut at the 300 ft level, we decided to make double layered walls at the 2000 ft site and build an PIR panel instrument box inside the isolated section of the tunnel. Again, a separate hut at some distance to the instrument area contains the PC and DC power supply. Whereas temperatures at the 300 ft level are strongly coupled to surface temperatures, the conditions at the 2000 ft level are more stable around $20°$C. By the end of the construction, a wired web link was produced between surface and the shaft at the 2000 ft level. The distance between our seismic station and Ross shaft is about 3000 ft which is too far to establish web access at our site via copper-ethernet link. A multimode optical fiber was ordered with transceiver units (copper-fiber transceiver) and switch since the link is shared with another science group. We had a lot of trouble to find the correct transceiver model, and lack of communication systems between our site and the shaft made it extremely cumbersome to configure the system and test the link. Details of the fiber system can be found in section 6.

Figure 14: Tunnel section at 2000 ft level.

5.3 The 800 ft site

The 800 ft site was built between September 2 and September 15. From all stations, most effort had to be dedicated to the 800 ft site. It is situated in a blind tunnel which used to store caps for explosives. No concrete platform existed, so that we had to build our own. About half a meter of

Figure 15: Pit to bottom rock at 800 ft site.

broken rock and mud formed the ground floor which had to be removed down to the rock at the end of the tunnel. After having shovelled a pit of $2 \times 1 \times 0.5$ cubic yards of soil, concrete was poured onto the rock to form a small horizontal platform for seismometers. PIR isolation was put up around the pit. A six-walled PIR cube at 4 m distance to the pit serves as computer hut. No power was available until the end of our visit, so that we could not install the instruments. Also, we expect that once we come back to this site, we will have to pour more concrete into the pit since water quickly formed a puddle at the ground which may rise higher than the concrete platform. We know where the water comes from and could block its way. The optical fiber between shaft and station was pulled, but there was no wired link yet from the surface to the 800 ft level.

6 Instrumentation

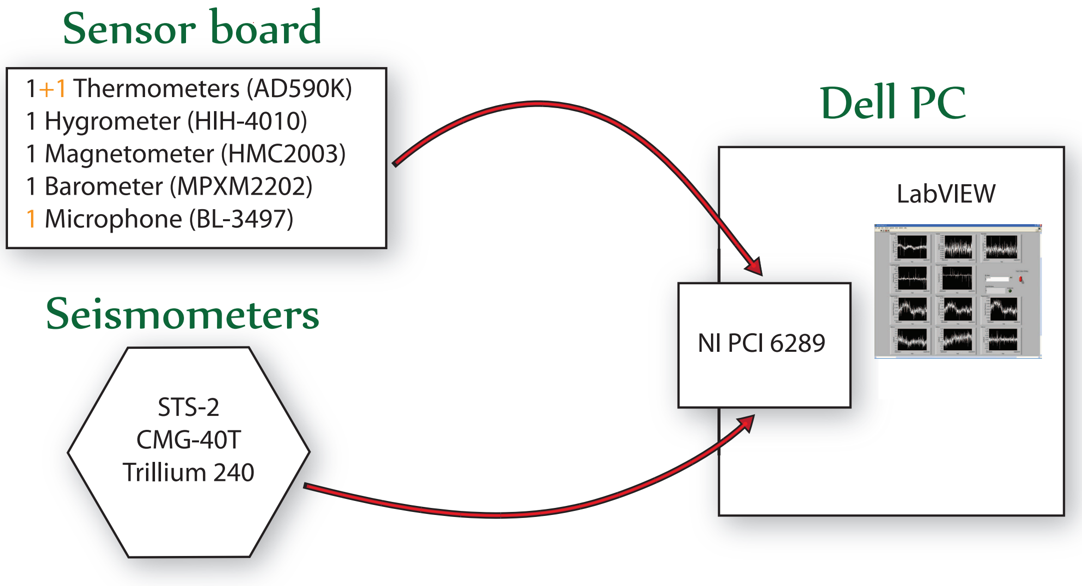

Figure 16: Sketch of instrument assembly used at each underground station. Orange numbers on the sensor board indicate that the respective sensors have not been used, but the circuit design would allow to implement them at any time.

6.1 Sensor board

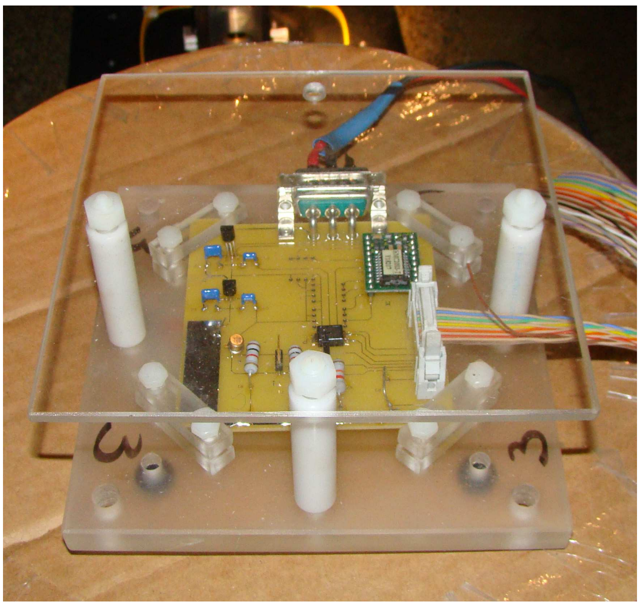

Figure 17: Sensor board as used at underground sites.

The sensor board monitors the environmental variables in the vicinity of the seismometers including temperature, pressure, humidity, sound, and the magnetic field (see figure 17). The microphone has not been used so far. The hygrometer may probably be spared at this point. Its purpose would be to warn the experimenter that humidity levels approach 100% and condensation of water on the electronics could start soon. So far, the sensor board operated reliably in highly humid environments ($\sim$ 90%). On mine levels with 100% humidity, isolation of the instrument hut was always good enough to bring humidity down to 80%-90%. Pressure and sound fluctuations may show significant correlation with seismic data since both could generate rock vibrations or may even directly act on seismometers despite all efforts to isolate the instruments. These sensors will become important as soon as one tries to understand a seismic spectrum in detail. The microphone may also be useful to identify and characterize man-made sources of seismic noise, e.g. measuring the spectrum near water pumps could reveal that part of the seismic spectrum is due to rock vibrations transmitted from pump to seismic stations. A similar analysis could be applied to the mine ventilation if one includes the pressure data. Most importantly, one has to monitor the temperature and magnetic field. The STS-2 and the current generation of Trilliums are sensitive to magnetic fields which is the dominant signal in seismic-noise measurements at low frequencies. Consequently, coherence between different instruments at low frequencies is also determined by the magnetic field and depends on magnetic susceptibilities of the instruments. We collected data which clearly show this effect (section 6.3). The temperature is known to be the dominant environmental factor which influences the response of seismometers. The pass band sensitivity of any seismometer which uses a NdFeB magnet decreases with increasing temperature by $-0.12\%/^{\circ}$C which is accompanied by a change in phase response according to the Kramers-Kronig relation. In correlation measurements, changes in the phase response can lead to loss of coherence.

6.2 Data-acquisition system

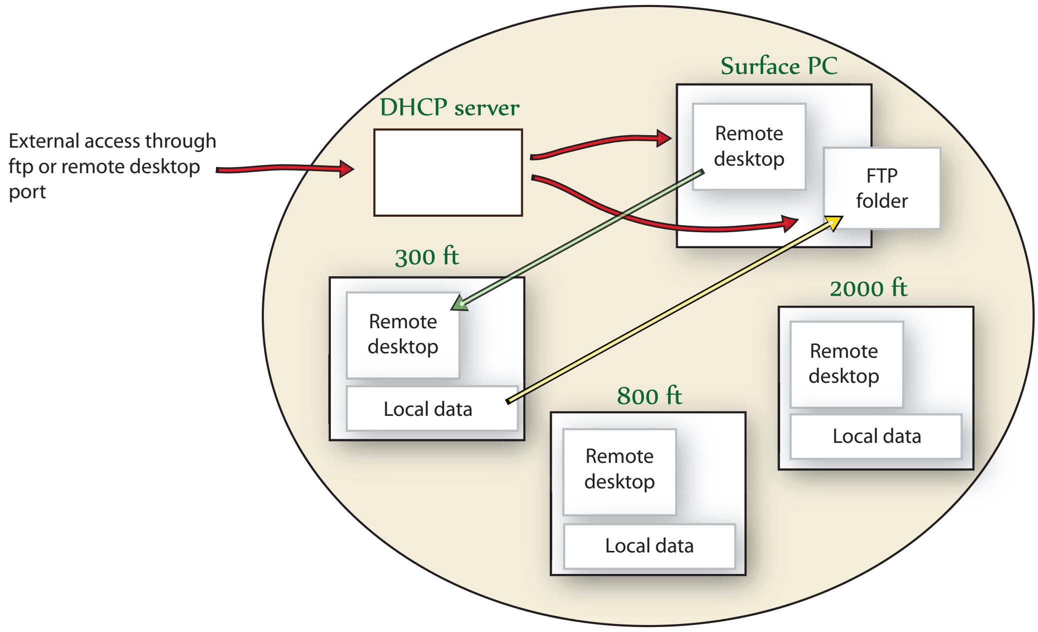

Figure 18: Sketch of the remote-access scheme and data acquisition. The system can be controlled remotely via the remote-desktop function. External users have to log into the surface PC. A second remote desktop can then be started on this machine to take control over the underground PCs. Data access is provided by a simple ftp server. A scheduled task copies data every 20 min from the underground stations to the ftp folder of the surface PC. A second scheduled task calls Matlab functions to down-sample some of the channels, before a virtual machine with Linux guest system retrieves the data (which is in ASCII format) and converts it into LIGO frames.

In this section, we describe the data-acquisition system which includes the configuration of the local network and remote access to our PCs. The acquisition system starts with the PCI 6289 card from National Instruments. It contains an 18bit ADC and an internal amplifier with maximal amplification of 100. The input range is limited to ± 10 V. Therefore, its nominal resolution is $80.1\,\mu$V assuming 5% over range and its highest resolution $0.8\,\mu$V. Two 68-pin VHDCI connectors support 32 analog inputs. Data acquisition is managed by LabVIEW programs which also generate analog-output signals to initiate mass-centering procedures of seismometers if necessary. The data is first stored in ASCII files as 128 s records sampled at 100 Hz. Eventually, data will be downsampled (except for the seismic and magnetometer channels) and converted into LIGO frames. The data is made available to the outside world by an ftp server. To run an ftp server, one has to manage remote access. We use a DHCP server which reserves an address range for static IPs. External requests through an ftp port are forwarded to the IP of the ftp server. Analogously, a second port is configured to forward remote desktop access to the same PC which is the surface PC inside the Ross Dry. Once logged onto this machine, one can use LAN-internal remote access to control the various underground stations, i.e. to start or stop DAQ or to copy data to the ftp folder. Underground web access is provided along the shaft by twisted-pair cables. Optical multimode fibers pick the signal from the twisted pair by media converters (multi-mode ST duplex to RJ45). These transceivers are specified up to 2000 m of multi-mode fiber length and are relatively inexpensive. A second pair of fibers has already been pulled at each level which will provide timing signals to all stations in the future. Currently, simple NTP demons are installed on all machines. The absolute timing may be relatively poor since typical timing errors (which cannot be corrected by the timing protocol) between the atomic-clock server (i.e. NIST time servers) and our surface PC typically exceed 30 ms. However, the relative timing between computers of our local network is about 0.2 ms and is at least for the moment sufficiently accurate.

Figure 19: Light Media Converter. It converts duplex ST into RJ45 (standard copper-ethernet connectors). A pair of transceivers is specified to transmit data over distances up to 2 km with 100Mbit/s.

6.3 Seismometers

Last summer, seismic data was produced from two different seismometer models: STS-2 and Trillium 240. In this section, we present models of the instrumental response and measured relative response functions between the STS-2 and the Trillium 240. Also, during a side-by-side measurement of two Trillium 240 and an STS-2, a three-channel analysis was carried out to obtain the instrumental noise spectra [5]. The poles and zeros of the response models are specified in table 1. The poles p_k and zeros z_k determine the complex response function T according to

$$T(f) = \frac{1}{\mathcal{N}} \frac{\prod\limits_k (i \cdot f + z_k)}{\prod\limits_k (i \cdot f + p_k)} \tag{1}$$

with $T(1\,\mathrm{Hz}) = 1$. A gain factor g in units [V/(m/s)] is multiplied after normalization. Values for each pole, zero and gain were taken from the respective manual. Figure 20 shows the absolute value and argument of the instrumental response eq. (1). Dividing the complex voltage amplitudes $\tilde{p}(f)$

Model	Poles [Hz]	Zeros [Hz]	Gain [V/(m/s)]
STS-2	$-0.0059 \pm 0.0059i$, -2.44, $-14 \pm 64.6i$, -66.5, -72.34, $-1514 \pm 1825.5i$, $-1629.7 \pm 433.7i$	$0, 0, -2.411, -32$, $-73.5 \pm 68.29i$	1500
T240	$-0.002889 \pm 0.002863i$, -27.53, $-31.19 \pm 36.76i$, $-116.5 \pm 225.2i$	$0, 0, -17.19, -25.62$	1196.5

Table 1: Response models of the STS-2 and Trillium 240.

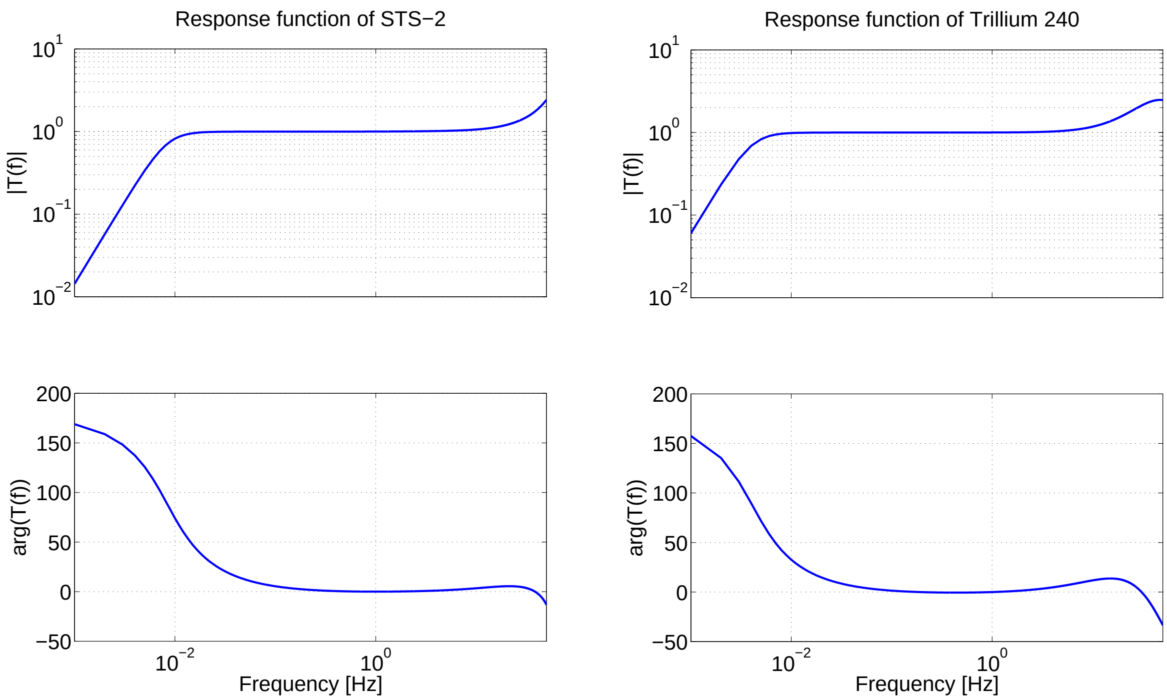

Figure 20: Amplitude- and phase-response models used in analyzing the data from the STS-2 and Trillium 240. Both response functions are normalized to $T(1\,\mathrm{Hz}) = 1$.

by the instrumental response, we obtain the modelled ground-velocity amplitudes $\tilde{v}(f)$:

$$\tilde{v}(f) = \frac{1}{g \cdot T(f)} \cdot \tilde{p}(f) \tag{2}$$

Whether models are good representations of the real response can be checked to some extent by calculating the relative transfer function $T_{12}(f)$ between two instruments according to

$$T_{12}(f) = \frac{\tilde{v}_1(f)}{\tilde{v}_2(f)} \tag{3}$$

where $\tilde{v}_1$, $\tilde{v}_2$ are the ground velocities derived from eq. (2) and data are obtained from a side-by-side measurement. Ideally, one should find $T_{12}(f) = 1$. The absolute value $|T_{12}|$ and phase $\arg(T_{12})$ for a side-by-side measurement of two Trillium 240 and one STS-2 is shown in figure 21. The ground velocities deduced from each instrument have identical amplitudes between 0.08 Hz and 4 Hz. However, a comparatively large difference is observed between the relative phases. To understand the

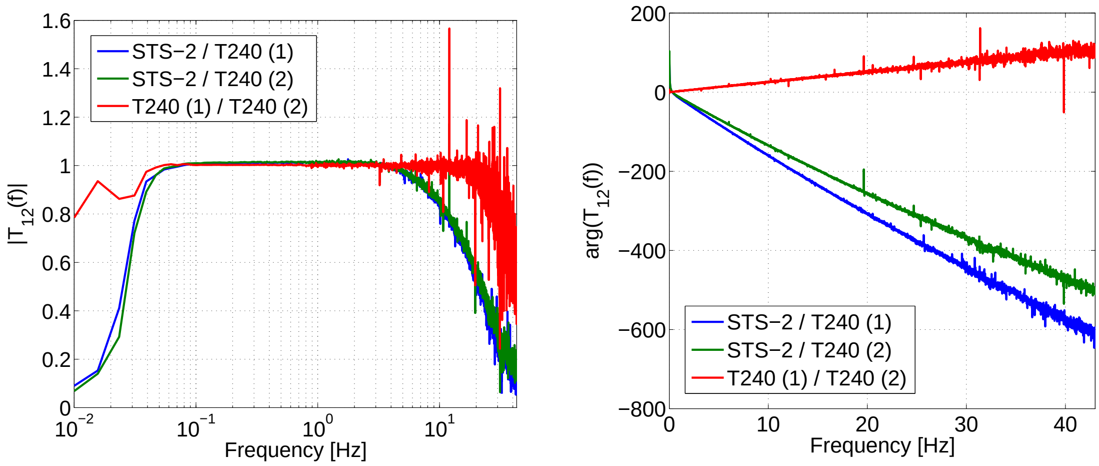

Figure 21: Absolute value and phase of the relative transfer function. Eq. (2) yields accurate results at all frequencies with high signal-to-noise ratio. At low frequencies the seismometers measured magnetic fields (with different susceptibilities) and at high frequencies instrumental self noise dominates the spectrum.

phase plots, one needs to know that the three seismometers were read out by three independent Taurus units which had been synchronized at surface and carried underground. Until the beginning of the measurement, a timing error $\Delta t_{\rm err}$ between clocks accumulated (e.g. due to temperature changes) which entails a relative phase shift between the amplitudes:

$$\begin{aligned}\tilde{p}_{\rm err}(f) &= \sum p(t)\mathrm{e}^{-2\pi i f(t+\Delta t_{\rm err})} \\ &= \tilde{p}(f)\cdot \mathrm{e}^{-2\pi i \Delta t_{\rm err} f}\end{aligned} \tag{4}$$

We need further analysis to explain the relative-amplitude spectra. The ground velocities modelled through the STS-2 data are weaker than the two T240 velocity spectra at frequencies below 0.08 Hz and above 4 Hz. The most likely causes are that either the T240 is susceptible to some environmental variable which the STS-2 is not, or the T240 is more noisy than the STS-2 or at least one of the response models is incorrect. At first, one can test whether the T240 spectra are dominated by self noise. Since three instruments participated in the measurement, self-noise spectra are evaluated by means of the three-channel technique as explained in [5]. This method is independent of the instrumental response which includes the applied model and the true response. The authors show that the spectral density of the self noise of instrument i can be estimated according to

$$S_i^{\rm n}(f) = S_i(f) - \frac{S_{ji}(f)\cdot S_{ik}(f)}{S_{jk}(f)} \tag{5}$$

Here, S_{ij} are the cross-spectral densities. In figure 22, we show the self noise together with measured seismic spectra in units of displacement. The lower triple of curves represent the self noise. The T240 has stronger estimated self noise at very low and very high frequencies. An increased susceptibility of the T240 to environmental variables cannot explain the noise spectra since any contribution to the data which is at least correlated between two instruments is subtracted (and leads to a higher noise estimate of the third instrument). Therefore, at very small frequencies it seems that the T240

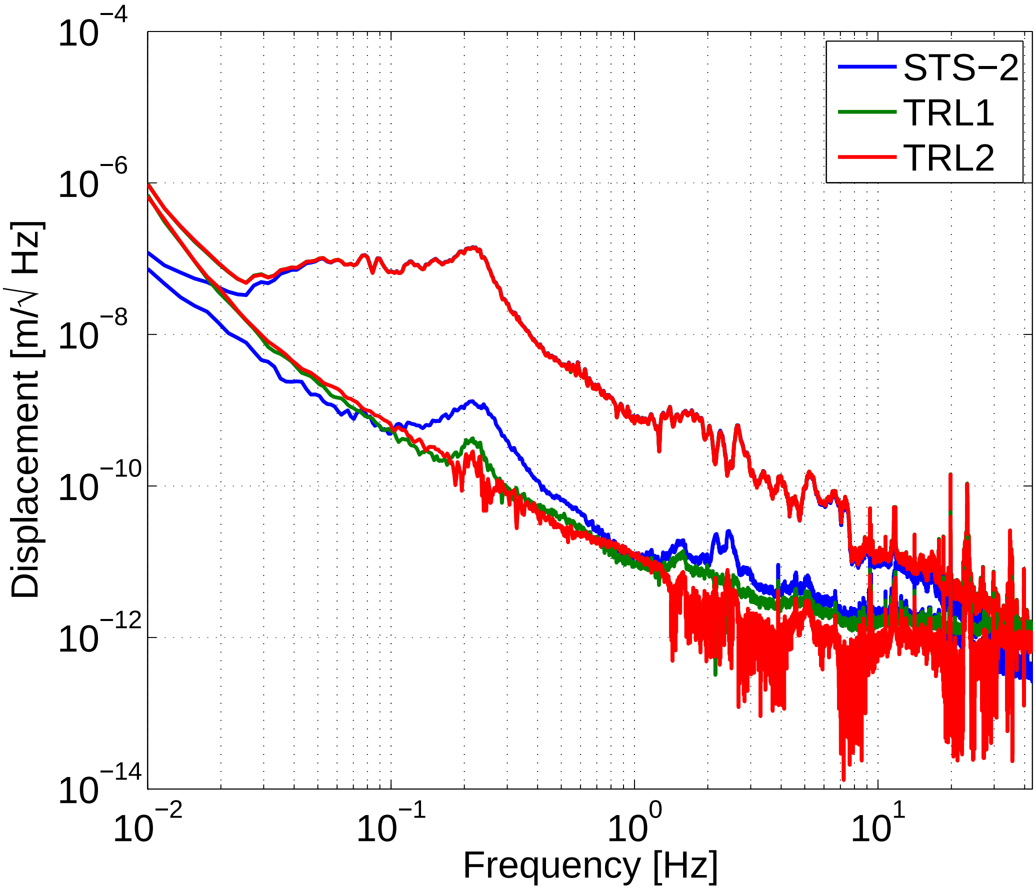

Figure 22: Comparison between the instrumental self noise and the measured displacement spectra. The self-noise estimate of the T240 is bigger than for the STS-2 at very low frequencies. The shadow of the microseismic peak on the self-noise curve may be due sliding on a rough surface or stress release of the instrument mounting caused by the microseismic wave itself.

is indeed more noisy which would also provide a sufficient explanation for the relative-amplitude spectra at those frequencies. At this point, we cannot conclude that the self noise of these two T240s is really worse than of the STS-2 which, in fact, is very likely not the case. For example, the three-channel method does not provide accurate self-noise estimates if the correlation between the instruments is poor. Plotting the coherence, we see that it is weak at the very frequencies which show high self noise (figure 23). Under these conditions, the method is based on incorrect assumptions and the self-noise estimate may even become dependent on the instrumental response. A candidate as a cause for the coherence loss at small frequencies is the instruments' susceptibilities to magnetic fields. If the magnetic susceptibility of the STS-2 was substantially different from the the one of the T240, then a coherence loss would be observed. Figure 24 displays the coherence between the seismometers and the magnetometer channel. Indeed, the correlation between the T240 and the magnetic field is stronger and may be the reason why we observe a smaller coherence between T240 and STS-2. Further theoretical investigations and experiments are needed to fully understand

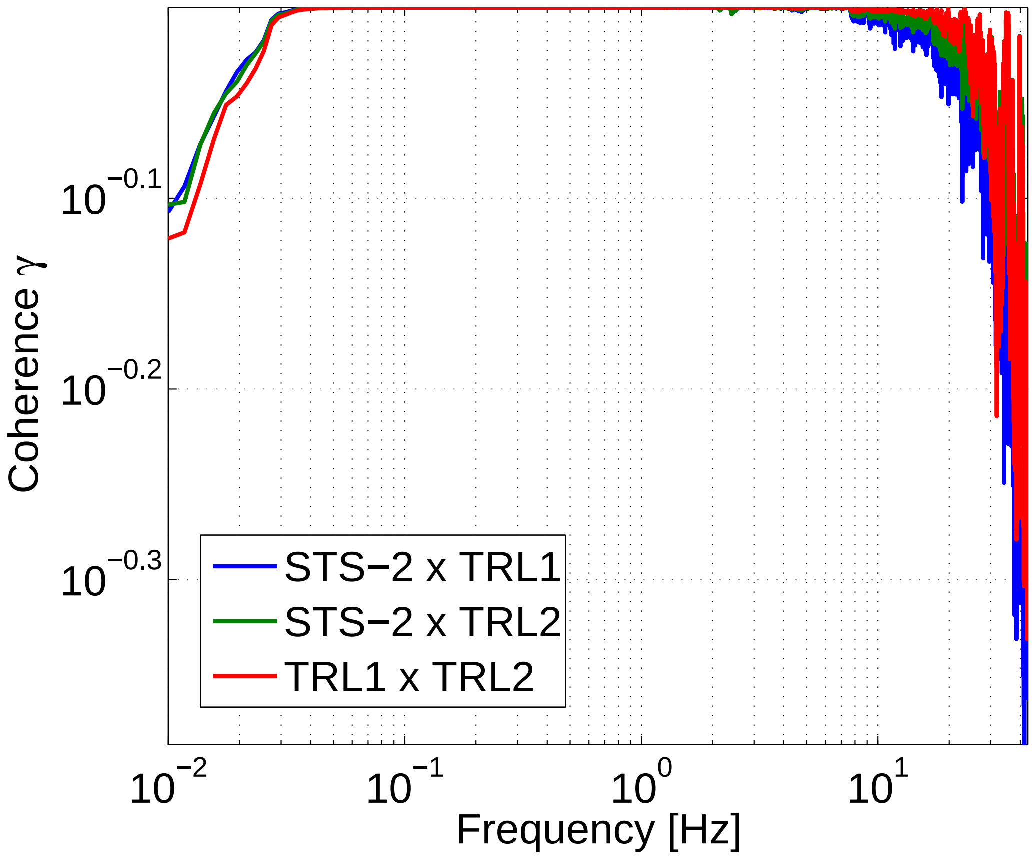

Figure 23: The decrease of coherence towards low frequencies is due to nonzero susceptibility to magnetic fields. The susceptibility has to be substantially different in at least one pair of instruments, otherwise coherence would still be close to one.

the data. Most fruitful would be a side-by-side measurement with three STS-2 and three Trillium 240. Then self-noise spectra could be compared using different combinations of instruments, also including combinations with three identical models. Other seismometers like the Güralp CMG-40T would be helpful to resolve similar problems at high frequencies.

7 Recent progress

We briefly outline the state of our experiment at the time we left Homestake in December 12:

- The 300 ft site is occupied by a Güralp CMG-40T. Environmental sensors are not operational for unknown reasons, but we suspect that the circuit board was destroyed by humidity.
- The 800 ft site is fully operational with an STS-2 and sensor board.
- The 2000 ft site is fully operational with a Trillium 240 and sensor board. In addition, Fausto Acernese has installed two seismometers aligned to a common horizontal direction which is read out in parallel with the other instruments by our DAQ system.

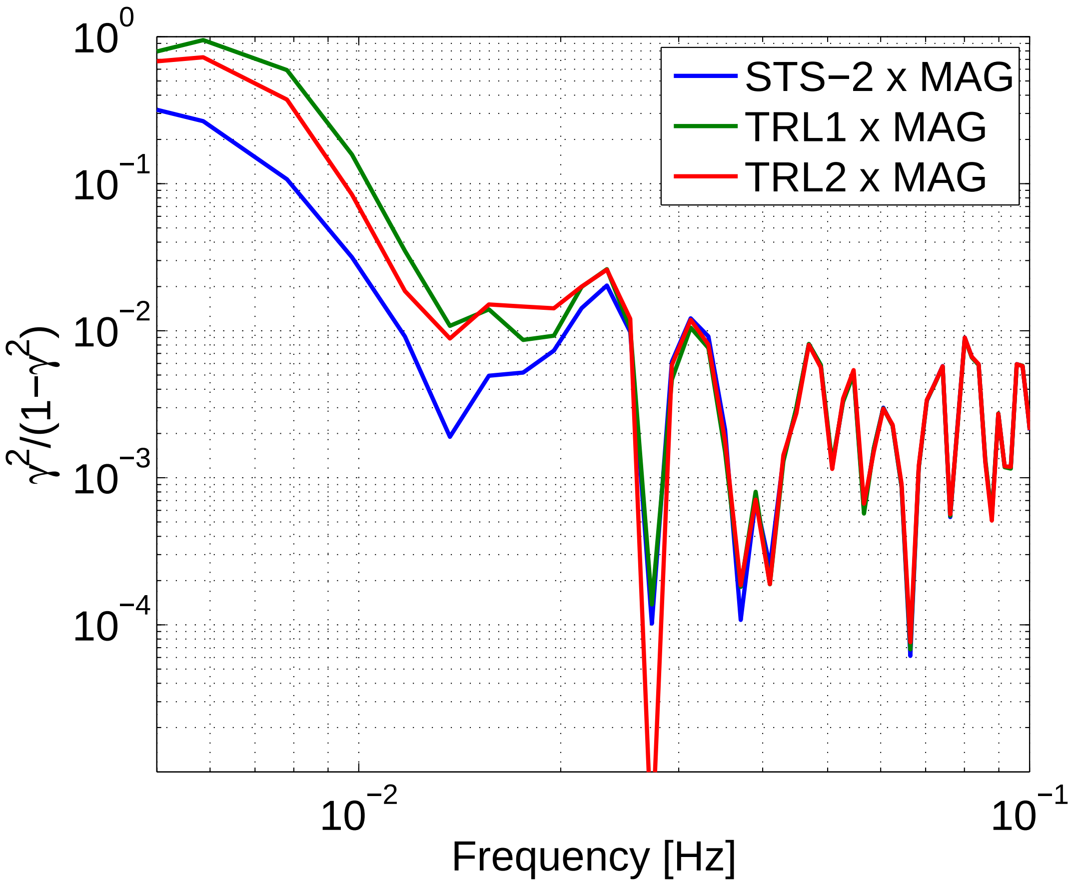

Figure 24: Coherence between seismometers and magnetic field.

- New data from all three stations is automatically uploaded to the ftp server at the surface

8 Acknowledgments

We thank LIGO for the kind support and loan of equipments, and hope to pay it back with exciting research. We would never have accomplished this work without the excellent support of the Sanford Lab. We are deeply grateful to everyone who worked with us. More recently, the new science-liaison director Jaret Heise has added further impetus and importance to our work. He always found a way to solve the unsolvable problems and was always eager to learn about our progress or failures. Next, we thank Gary Lillehaug. Without him, our stations would still be in darkness and disconnected from the world. His support was invaluable. We also found new friends and colleagues at Homestake. We say thank you to Prof Bill Roggenthen who provided us with all necessary information of the Homestake geology, and his student Jason van Beek who helped us many days with setting up the underground network. We hope that our ways will cross regularly in the future. The same is true for Nick Ackerley who was our guest for one week. His support goes well beyond his duties as a representant of the Nanometrics company. Nobody could have taught us more about how to set up a seismic measurement. In endless discussions, he has helped us to debug and understand our analysis code. Finally, we thank Szabolcs Marka who introduced us to the methods of clock synchronization which is so important for our experiment, and our guest Vinzenz Wand who came to us at a time when his helping hand was more than welcome.

References

[1] E. DeWitt, J. A. Redden, D. Buscher, and A. Burack Wilson. Geologic Map of the Black Hills Area, South Dakota and Wyoming. *USGS Miscellaneous Investigations Series*, 1989.

[2] F. Acernese et al. Seismic stations implementation and improvements at Homestake. *LIGO document*, page T080344, 2008.

[3] J. A. Noble and J. O. Harder. Stratigraphy and metamorphism in a part of the nothern Black Hills and the Homestake mine, Lead, South Dakota. *Bull. Geo. Soc. Am.*, 59:941, 1948.

[4] S. W. Caddey et al. The Homestake Gold Mine, An Early Proterozoic Iron-Formation-Hosted God Deposit, Lawrence County, South Dakota. *Geo. Survey. Bull.*, 1991.

[5] R. Sleeman, A. van Wettum, and J. Trampert. Three-Channel Correlation Analysis: A New Technique to Measure Instrumental Noise of Digitizers and Seismic Sensors. *Bull. Seism. Soc. Am.*, 96:258, 2006.